Analyzing the impact of design factors on external walls in lightweight modular construction based on life-cycle analysis

Energy, economic, and environmental trade-offs

Hu, Yan; Ai, Zhengtao; Zhang, Guoqiang; Zong, Jie; Liu, Zhengxuan

DOI
10.1016/j.jobe.2025.112090

Publication date
2025

Document Version
Final published version

Published in
Journal of Building Engineering

Citation (APA)
Hu, Y., Ai, Z., Zhang, G., Zong, J., & Liu, Z. (2025). Analyzing the impact of design factors on external walls in lightweight modular construction based on life-cycle analysis: Energy, economic, and environmental trade-offs. *Journal of Building Engineering*, *103*, Article 112090. https://doi.org/10.1016/j.jobe.2025.112090

Journal of Building Engineering 103 (2025) 112090

Contents lists available at ScienceDirect

Journal of Building Engineering

journal homepage: www.elsevier.com/locate/jobe

Analyzing the impact of design factors on external walls in lightweight modular construction based on life-cycle analysis: Energy, economic, and environmental trade-offs

Yan Hu [a], Zhengtao Ai [a,b,*], Guoqiang Zhang [a,b], Jie Zong [a], Zhengxuan Liu [a,b,c]

[a] Department of Building Environment and Energy, College of Civil Engineering, Hunan University, Changsha, Hunan, 410082, China
[b] National Center for International Research Collaboration in Building Safety and Environment, Hunan University, Changsha, Hunan, 410082, China
[c] Faculty of Architecture and the Built Environment, Delft University of Technology, Julianalaan 134, 2628 BL, Delft, the Netherlands

ARTICLE INFO

Keywords:
Muti-objective optimization
External wall
Life-cycle analysis
Optimal thickness
Lightweight modular integrated construction

ABSTRACT

One significant challenge in lightweight modular integrated construction (MIC) is to determine the optimal performance of external wall to minimize life-cycle energy consumption, economic costs, and environmental impact (3E). This study compares 3E-objective and single-objective optimization methods for determining the optimal thickness of MIC across five distinct climatic zones in China. Additionally, it analyzes how factors like heating, ventilation, and air conditioning (HVAC) operational duration, climate change, grid emission factors, and building lifespan affect the optimal thickness. Results reveal that the 3E-objective optimization method achieves the highest cost-benefit ratio in carbon reduction, outperforming the energy or environmental method. Lightweight external walls, with low thermal mass, have an optimal thickness deviating from the current nearly zero-energy building standard, with deviations reaching up to 200 mm in optimal thickness. Reduced HVAC operational duration, global warming, decreased grid emission factors, and extended building lifespan contribute to a potential reduction in the optimal wall thickness by up to 140 mm. These deviations in the configuration of these factors, although they may lower life-cycle cost investments compared to the optimal thickness, could potentially be unfavorable or detrimental to reduce life-cycle energy consumption and carbon emissions. The deviation in HVAC operational duration exhibits the most significant impact on life-cycle 3E results, reaching up to 8.4 %. Climate change has a relatively minimal impact on the life-cycle 3E results. This research can advance the cost-benefit ratio in carbon emission reduction of MIC and highlight the need for flexible building standards to accommodate climatic and operational variations.

Nomenclature	
A	Total wall area (m^2)
C	Initial investment per unit weight (CNY/kg)
$C_{op,n}$	Operational costs in the n year (CNY)
C_t	Total economic costs (CNY)

(*continued on next page*)

* Corresponding author. Department of Building Environment and Energy, College of Civil Engineering, Hunan University, Changsha, Hunan, 410082, China.

E-mail address: zhengtaoai@hnu.edu.cn (Z. Ai).

https://doi.org/10.1016/j.jobe.2025.112090
Received 25 October 2024; Received in revised form 6 February 2025; Accepted 10 February 2025
Available online 11 February 2025

(*continued*)

CO_2	Embodied carbon emissions per unit weight (kg·CO_2/kg)
CO_{2em}	Total embodied emissions (kg·CO_2)
$CO_{2op,n}$	Operational carbon emissions in the n year (kg·CO_2)
CO_{2t}	Total carbon emissions (kg·CO_2)
EE	Embodied energy per unit weight (MJ/kg)
EF	Carbon emission factor for electricity (kg·CO_2/kWh)
E_t	Total energy consumption (MJ)
EU_n	Annual energy electricity consumption in the n year (kWh)
EU_0	Annual energy electricity consumption of the reference year (kWh)
g	Growth rate
i	Interest rate
k	Inflation rate
L	Thickness (mm)
l	Loss rate
M	Total mass of the material (kg)
N	Building lifetime
n	year counter
r	Number of material replacement
α	Cost per unit of electricity (CNY/kWh)
$X_{j,d}$	Dimensionless number of the evaluation parameter ,$E_{t,d}$, $C_{t,d}$, and $CO_{2t,d}$
$X_{j,d,min}$	Minimum dimensionless number of the evaluation parameter
X_j	Evaluation parameter, E_t, C_t, and CO_{2t}
$X_{j,opt}$	Evaluation parameters corresponding to the optimal thickness
$X_{j,opt,base}$	Evaluation parameters corresponding to the optimal thickness for the operating baseline
Y_d	Dimensionless trade-off Pareto frontier
$Y_{d,opt}$	Dimensionless unique optimal solution
Subscript	
em	Embodied
gal	Galvalume sheet
insul	Insulation material
opt	Optimal solution
op	Operational
t	Total
Abbreviations	
EPS	Expanded polystyrene
HSCW	Hot summer cold winter
HSWW	Hot summer warm winter
HVAC	Heating, ventilation, and air conditioning
MAE	Mean absolute error
MIC	Modular integrated construction
nZEB	Technical standard for nearly zero energy buildings
RMSD	Root mean bias error
SC	Severe cold
SSP	Shared socioeconomic pathway
XPS	Extruded polystyrene
COP	Coefficient of performance

1. Introduction

The global building sector plays a crucial role in mitigating global warming with 34 % global energy demand and 37 % related carbon emissions in 2022 [1]. Recent studies have revealed the growing significance of embodied energy and carbon emissions associated with building material production and processing, yet their significance is often underestimated in life-cycle analysis [2].

The external wall plays a crucial role in minimizing embodied and operational energy consumption in buildings. Determining the optimal design for external wall is imperative for mitigating global climate change, enhancing energy efficiency, and reducing economic costs [3].

In earlier studies, most researchers employed single-objective optimization techniques to explore the optimal insulation thickness based on energy efficiency analysis [4–6]. Given the global drive towards carbon neutrality and recent revisions in building regulations, an increasing number of researchers have commenced integrating carbon emissions studies into this field [3,7–9]. The environmental payback periods for the use of insulation materials are much shorter than economic ones. This reveals the environmental importance of thermal insulation in buildings [3]. The optimum insulation thickness calculated through the environmental criteria results, in some cases, 10 times higher than the one calculated through the economic criterion [7,8]. When faced with uncertainties surrounding energy decarbonization in specific cities, this more cautious approach involving over-investment based on environmental impact may be recommended [10]. Obviously, such an approach is not always suitable. Several studies have considered multi-objective trade-offs, including one or more of economy, energy, electricity tariff, or thermal comfort [3,11–13]. In the process of multi-objective optimization, the setting of parameters plays a crucial role in determining the optimization solutions. As indicated by the literature review, the optimal thickness of external wall is contingent upon a multitude of parameters, including building operational mode [14,15], climatic conditions [13,16–19], grid emission factors [9,17], building lifespan [8], and other parameters [20].

The setting of these parameters may deviate from national standards or codes, such as the technical standard for nearly zero energy buildings GB/T51350 [21].

When evaluating multiple objectives such as economic costs, energy consumption, and carbon emissions (3E) during both the embodied and operational phases of buildings, conflicts often arise among these objectives. Multi-objective optimization methods have been proven to be effective in addressing such conflicts. Notably, the Non-dominated Sorting Genetic Algorithm (NSGA-II) has been successfully employed by researchers to formulate multi-objective optimization problems and is widely acknowledged as one of the most efficient genetic algorithms [22]. Li et al. [13] utilized NSGA-II to seek the optimal Pareto set among the three objective functions of heating demand, cooling demand, and global cost, demonstrating great potential in enhancing building energy efficiency. Naji et al. [20] carried out the optimization of envelope parameters using the NSGA-II algorithm. Wu et al. [12] used the NSGA-II algorithms to optimize the design of residential buildings in hot summer and cold winter regions with respect to energy consumption, thermal comfort, and daylighting performance, incorporating the ideal point method to determine the optimal combination of building

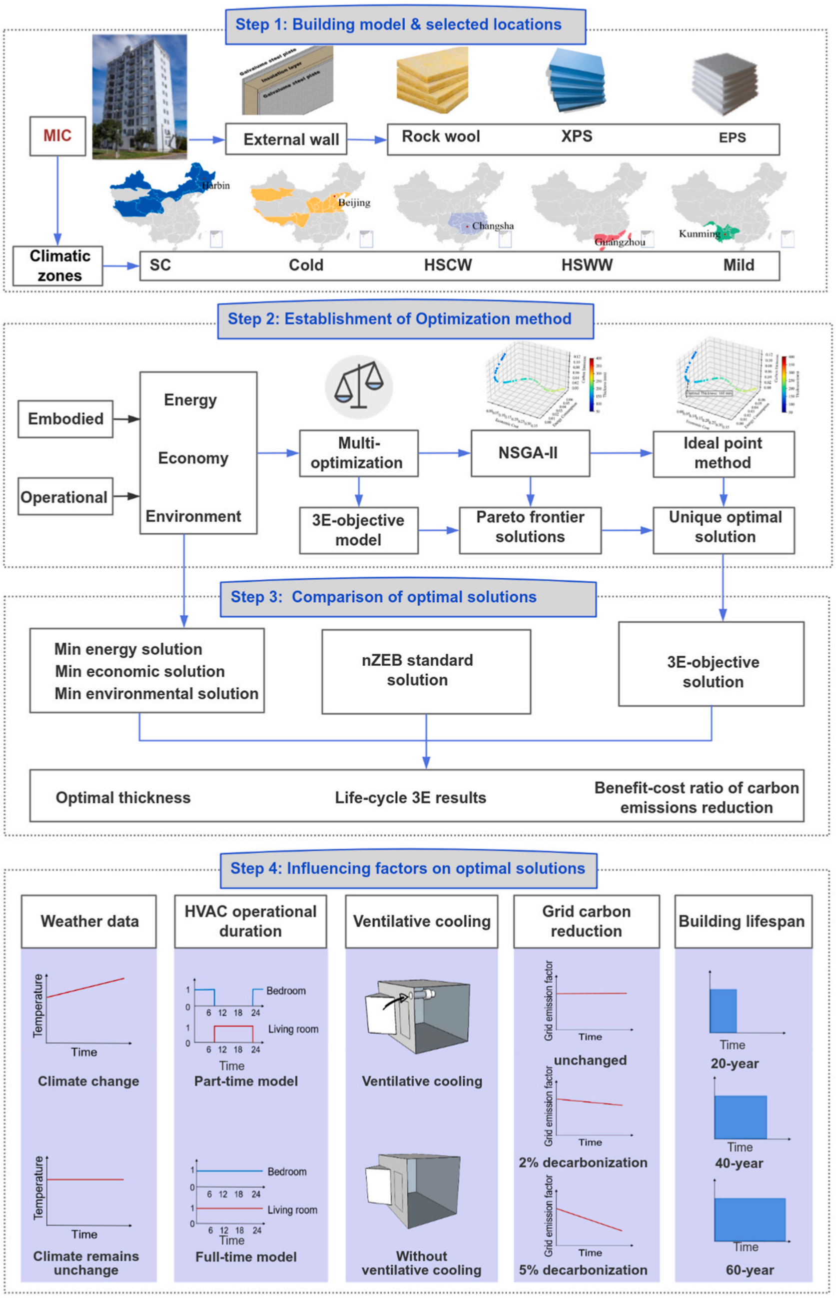

Fig. 1. Research workflow.

parameters from the Pareto frontier. The ideal point method is a decision-making technique used to evaluate and select the optimal solution that is closest to the ideal point, thereby determining the best combination of building parameters.

Based on the authors' current review, no research has delved into the optimization of external wall in lightweight Modular Integrated Construction (MIC). MIC represents a distinctive off-site construction approach, which can significantly reduce the average embodied carbon emissions by 15.6 % [23] and life-cycle costs by 21 % [24], compared to traditional construction methods. Typically, MIC utilizes lightweight and durable materials as opaque envelopes, such as sandwich panel systems or wood-framed systems [25]. There are significant differences in both composition and energy characteristics between lightweight MIC envelopes and traditional heavyweight building envelopes [23,26–28]. The use of these lightweight envelopes has increased operational energy consumption and carbon emissions [23,26–28]. Nevertheless, it remains uncertain whether such an increase will occur in different climatic zones and under the scenario of future climate change according to the previous comparative energy performance studies [29]. No studies have systematically examined the trade-offs between embodied and operational energy, economic costs, and carbon emissions specific to the external wall of lightweight MIC. Additionally, the potential deviation of the optimized thickness caused by incorrect parameter settings during the optimization process, and its positive or negative impact on economic benefits, energy efficiency, and carbon emissions over the whole life cycle have yet to be explored.

This paper aims to contribute to the development of MIC towards reduced life-cycle energy consumption, economic costs, and carbon emissions associated with MIC's external wall. The novelty of this study lies in the following.

- A comprehensive examination is conducted on the embodied and operational energy, economic, and environmental aspects of the external wall of lightweight MIC.
- An optimization approach integrating NSGA-II and the ideal point method is adopted to determine the optimal thickness of external wall, balancing the trade-offs among life-cycle economic costs, energy consumption, and carbon emissions.
- The effect of deviations in the settings of HVAC operational mode, future climate change scenarios, grid carbon emission factors, and building lifespan on the selection of the optimal thickness of external wall during the 3E-objective optimization process, as well as on the life-cycle 3E results is explored.

2. Methods

The study employed a representative lightweight MIC in China as the building model to investigate the optimal thickness of external wall. Firstly, models for the energy, economic, and environmental aspects of the building's external wall, as well as the 3E-objective optimization method were established. Then, an analysis of the comparative results of optimization attained through various single-objective optimization methods and 3E-objective optimization methods was presented. Finally, the influence of various factors in the process of external wall optimization on the optimal thickness was analyzed. The research workflow employed in this study is depicted in Fig. 1.

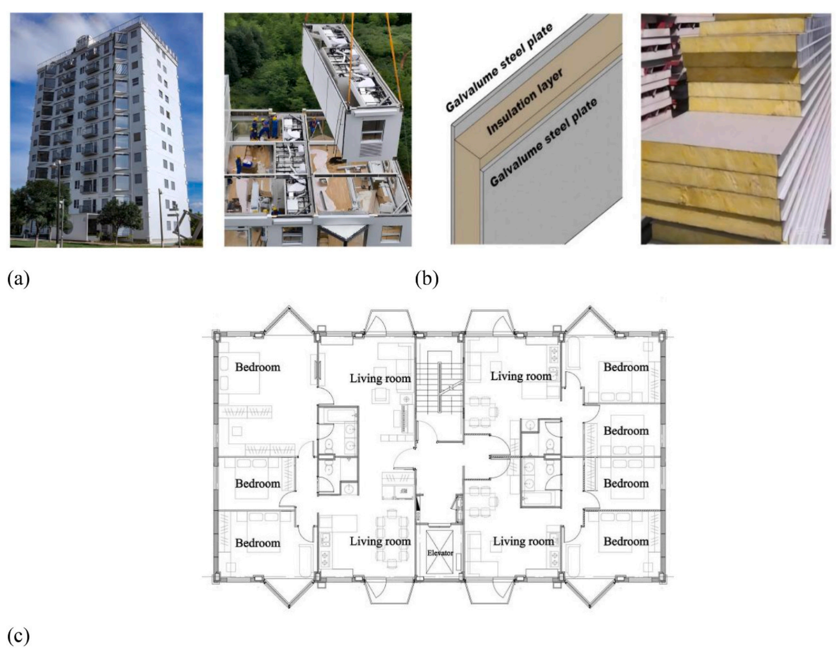

Fig. 2. (a) Baseline building, (b) the external wall in MIC, and (c) its floor plan layout.

2.1. Building model and selected locations

The baseline building used in this study was a representative MIC located in Changsha, China. It was a multi-story residential building with a total floor area of 2968 m^2 and an average height of 33 m. Fig. 2 depicts an overview of the selected building, including its external wall structure and floor plan layout. The external wall was constructed using an innovative sandwich panel system consisting of a low-density core and two rigid coatings, thereby constituting a lightweight envelope. This external wall design facilitates energy-efficient practices within the construction industry while promoting the development of environmentally friendly buildings [30].

In this study, three types of lightweight sandwich panel systems with commonly used core materials were evaluated: rock wool, expanded polystyrene (EPS), and extruded polystyrene (XPS). Table 1 shows the physical properties of the sandwich panel system materials. The primary thermal performance was attributed to the insulation material in the core layer. The sandwich panel system is commonly used in applications where the core layer thickness exceeds 50 mm [31]. In addition, it is essential to consider that excessively thick walls may impede the efficient space utilization within the structure. For our research, a range of thickness from 50 mm to 400 mm, with an increment of 50 mm, was considered. This range complies with GB/T51350 [21] across all climatic zones. Five climatic zones of China were selected, namely severe cold (SC), cold, hot summer and cold winter (HSCW), hot summer and warm winter (HSWW), and mild. Five representative cities in these zones were chosen for detailed analysis. Table 2 shows the thermal performance of the external wall and the thickness range of the corresponding insulation layer based on GB/T51350 [21] in the five selected cities.

2.2. Optimization method

The present section outlines the detailed life-cycle energy, economic, and environmental models, followed by the optimization procedure for achieving 3E-objective.

2.2.1. Energy model

The primary focus of this investigation lies in examining the energy consumption associated with both embodied energy of external wall materials and operational energy usage related to HVAC systems. Embodied energy consumption is defined as the total amount of primary renewable and non-renewable energy utilized in extracting raw material sources, transportation, processing, and production of selected building materials. The total mass of external wall material can be calculated by Eq. (1) and Eq. (2) [32]:

$$M_{gal} = A \times \rho_{gal} \times L_{gal} \tag{1}$$

$$M_{insul} = A \times \rho_{insul} \times L_{insul} \times (1 + r) \times (1 + l) \tag{2}$$

where M_{gal} and M_{insul} are the masses of galvalume sheet and insulation material, ρ_{gal} and ρ_{insul} are the densities of galvalume sheet and insulation material, L_{gal} and L_{insul} are the thicknesses of galvalume sheet and insulation material, A is the total external wall area, r is the number of insulation material replacement during the entire lifespan of the building, and the lifespan of insulation material is assumed to be 20 years, and l is fractional loss rate of the insulation material during the construction, which is assumed to be 5 % here.

For operational energy, once the site energy was calculated, it was converted to primary or source energy savings using a site-to-source conversion factor of 3.6 MJ/kWh [33].The total energy consumption E_t during life cycle was calculated by Eq. (3):

$$E_t = 3.6\sum_{n=1}^{N} EU_n + \left(EE_{gal} \times M_{gal} + EE_{insul} \times M_{insul}\right) \tag{3}$$

where EU_n is the annual energy electricity consumption related to HVAC in the n year, N is the building lifetime, and EE_{gal} and EE_{insul} refer to the embodied energy per unit weight of galvalume sheet and insulation material.

2.2.2. Economic model

The economic model includes the initial and replacement investment associated with external wall materials, as well as the operational costs related to HVAC systems over a specified lifetime. Considering the time value of economic costs is crucial in evaluating project financial feasibility and long-term profitability. The annual operational costs $C_{op,n}$ in the n year and total economic costs C_t during life cycle were calculated according to the following Eq. (4) and Eq. (5) [7], respectively:

$$C_{op,n} = EU_n \times \alpha \tag{4}$$

Table 1
Physical properties of the sandwich panel materials.

Materials	Thermal conductivity (W/(m·K))	Density (kg/m^3)	Specific heat capacity (kJ/kg·K)
Rock wool	0.041	140	1.22
XPS	0.032	40	1.40
EPS	0.040	30	1.40
Galvalume sheet	58.200	7850	0.48

Table 2
Thermal performance of the external wall and the thickness range of the corresponding insulation layer according to nZEB standard GB/T51350 [21].

Cities (Climatic zones)	Latitudes	climatic zones		Thermal transmittance of external wall ($W/m^2 \cdot K$)	Thickness range based on nZEB standard (mm)		
		Chinese	Köppen-Geiger		Rock wool	XPS	EPS
Harbin (SC)	45°45′	SC	Dwa	0.10–0.15	265–400	208–300	260–395
Beijing (Cold)	39°54′	Cold	Dwa	0.15–0.20	190–265	150–208	193–260
Changsha (HSCW)	28°12′	HSCW	Cfa	0.15–0.40	96–265	75–208	94–260
Guangzhou (HSWW)	23°08′	HSWW	Cfa	0.30–0.80	45–130	35–100	44–126
Kunming (Mild)	25°02′	Mild	Cwb	0.20–0.80	45–190	35–150	44–193

$$C_t = \left(C_{gal} \times M_{gal} + C_{insul} \times M_{insul}\right) \times (1+i)^N + \sum_{n=1}^{N} C_{op,n} \times (1+i)^{N-n} \times (1+k)^{n-1} \quad (5)$$

where C_{gal} and C_{insul} are the initial investments of per unit weight of galvalume sheet and insulation material, i is the interest rate, k refers to the inflation rate, and α is the cost per unit of electricity.

2.2.3. Environmental model

The comprehensive life-cycle carbon emissions encompass an evaluation of embodied carbon emissions associated with external wall materials and operational carbon emissions related to HVAC systems. The total embodied emissions CO_{2em} and operational carbon emissions $CO_{2op,n}$ in the n year were calculated by Eq. (6) and Eq. (7), respectively, and the total carbon emissions CO_{2t} during life cycle was calculated using Eq. (8):

$$CO_{2em} = CO_{2gal} \times M_{gal} + CO_{2insul} \times M_{insul} \quad (6)$$

$$CO_{2op,n} = EF \times EU_n \quad (7)$$

$$CO_{2t} = \sum_{n=1}^{N} CO_{2op,n} + CO_{2em} \quad (8)$$

where CO_{2gal} and CO_{2insul} are the embodied carbon emissions per unit weight of galvalume sheet and insulation material, and EF refers to carbon emission factor for electricity.

The specific parameter configurations in the energy, economic, and environmental models are presented in Table 3.

2.2.4. 3E-objective optimization method

The above 3E models, encompassing energy, economy, and environment, should be dimensionless to facilitate standardized comparisons on a consistent scale, as demonstrated in Eq. (9):

$$X_{j,d} = \left(X_j - X_{j,min}\right) / \left(X_{j,max} - X_{j,min}\right) \ \left(0 \le X_{j,d} \le 1\right) \quad (9)$$

where $X_{j,d}$ is the normalized dimensionless function of X_j, X_j is the evaluation parameter, such as E_t, C_t, and CO_{2t}. $X_{j,max}$ and $X_{j,min}$ are the maximum and minimum values of evaluation parameters.

The 3E-objective optimization method was to identify a good trade-off Pareto frontier Y_d that can achieve the best balance among three dimensionless indicators throughout the entire life cycle, which can be expressed in Eq. (10):

$$\min \ Y_d = \left(E_{t,d}, C_{t,d}, CO_{2t,d}\right) \quad (10)$$

where $E_{t,d}$, $C_{t,d}$, and $CO_{2t,d}$ are the objective functions that need to be optimized, which are the normalized dimensionless functions of

Table 3
Parameters utilized in the calculations [7,34–38].

Parameters	Units	Values	Parameters	Units	Values
i	%	4.9	α	CNY/kWh	0.547
k	%	2.56	N	Year	60
C_{insul}-Rock wool	CNY/m^3	420	CO_{2insul} -Rock wool	$kg \cdot CO_2/kg$	1.05
C_{insul}-XPS		620	CO_{2insul} -XPS		3.45
C_{insul}-EPS		320	CO_{2insul} -EPS		2.55
C_{gal}	CNY/kg	4160	CO_{2gal}		0.96
EF-Harbin	$kg \cdot CO_2/kWh$	0.6342	EE_{insul} -Rock wool	MJ/Kg	16.8
EF-Beijing		0.5688	EE_{insul} -XPS		109.2
EF-Changsha		0.5138	EE_{insul} -EPS		88.6
EF-Guangzhou		0.4715	EE_{gal}		17.6
EF-Kunming		0.1235			

E_t, C_t, and CO_{2t} calculated by Eq. (9), respectively.

The NSGA-II is a method that utilizes non-dominated sorting, crowding distance calculation, and selection operations to tackle the challenges of searching and maintaining the Pareto frontier, thereby enhancing computational efficiency and convergence rate. The NSGA-II algorithm iteratively adjusts the energy, economic, and environmental objective values based on the performance simulation results of the model to generate multiple combinations of morphological parameters for exploring Pareto optimal solutions. In the decision-making process, these three objectives were treated equally and assigned the same weight in this study. Table S1 in the Supplementary Information (SI) file presents the algorithm parameters and their corresponding values for the multi-objective optimization.

A set of trade-off solutions consistent with the Pareto optimal state decision variables was calculated by NSGA-II, instead of a unique optimal solution. The ideal point method [12] was employed to select the most suitable solution from the non-dominated options on the Pareto frontier, to help decision-makers identify the optimal solution that considers all objectives equally important. Eq. (11) was used to calculate the distance between each solution and the ideal point, thereby determining the minimum distance as the dimensionless unique optimal solution $Y_{d,opt}$.

$$Y_{d,opt} = \min\sqrt{\sum_{j=1}^{3}\left(X_{j,d} - X_{j,d,min}\right)^2} \tag{11}$$

Where $X_{j,d,min}$ is the minimum dimensionless number of the evaluation parameter.

Finally, the obtained dimensionless unique optimal solution was used to inverse-calculate each evaluation parameter through Eq. (9), and then the optimal thickness corresponding to the evaluation parameter value was calculated by interpolation method.

2.3. *Influencing factors*

The optimal thickness of external wall is influenced by multiple factors, primarily including building operational parameters and external climatic variations. The subsequent sections will elaborate on the details of these factors.

2.3.1. *Building operating conditions*

The entire residential building was selected for analysis. Two HVAC operational duration modes were considered: full-time and part-time. The full-time mode referred to the continuous operation of the HVAC system throughout the entire space all day, ensuring maintenance of thermal comfort at a comfortable level and indoor air quality at an acceptable level for the entire space. In contrast, the part-time mode adopted a local space and time-sharing operational strategy, enhancing its energy efficiency. Table 4 shows the parameters in the energy calculation model.

The energy-saving measure of adopting ventilation for cooling technology (referred to as ventilation cooling) has been compared. The control strategy for ventilative cooling, which involves a mechanical ventilation airflow rate of 2 air changes per hour, was derived from the previous research [29]. For the baseline case without ventilative cooling, the set temperature for heating and cooling indoor air is 20 °C and 26 °C, respectively.

This study selected three different building lifespans of 20 years, 40 years, and 60 years for comparison. During the building lifespan, three alternative grid technology scenarios were established: a baseline scenario with an unchanged grid emission factor, a dynamic scenario with a 2 % decrease annually in the grid emission factor (referred to as the 2 % decarbonization model), and another dynamic scenario with a 5 % decrease annually in the grid emission factor (referred to as the 5 % decarbonization model) [10]. Table 5 summarizes the optimization scenarios of this study.

2.3.2. *Climate change and energy demand calculation*

Considering the effect of future climate change, the future weather data for the 2050s and 2080s were predicted using the Future Weather Generator (https://adai.pt/future-weather-generator) [40], which enables the forecasting of building energy consumption. The current weather data records were obtained from the climate.onebuilding.org website, covering a period from 2004 to 2018 [40]. Building energy simulations were conducted via the EnergyPlus platform [7] to estimate the current and future operational energy consumption.

Fig. 3 shows the evolution model of energy demand for cooling and heating. To more accurately reflect energy consumption trends, segmented calculations of the annual growth rate of energy consumption for each period were performed, and interpolation of energy consumption for intermediate years was carried out using these growth rates by Eq. (12). This process aims to derive precise predicted values for HVAC energy consumption [41].

Table 4
Parameters in the energy calculation model [39].

Inputs	Values
HVAC system operating hours	8:00–21:00 for living room; 22:00–7:00 for bedroom
Internal heat sources	Lighting: 5 W/m^2; People: 120 W/person; Equipment: 3.8 W/m^2
Minimum fresh air	30 m^3/h per person

Table 5
Variable settings in the optimization scenarios.

Influencing factors	Related variable settings	Additional description
Weather Files (15 options)	1) Taiping international airport 2) Beijing capital international airport 3) Huanghua international airport 4) Baiyun international airport 5) Wujiaba international airport	Regard climate change as the operating baseline
Sandwich panel systems (24 options)	1) Rock wool 2) EPS 3) XPS	A range of thickness from 50 mm to 400 mm, with an increment of 50 mm
HVAC operational mode (3 options)	1) Full-time mode without ventilative cooling 2) Part-time mode without ventilative cooling 3) Full-time mode with ventilative cooling	Operating baseline
Building lifespans (3 options)	1) 60 years 2) 40 years 3) 20 years	Operating baseline
Grid carbon reduction mode (3 options)	1) Static grid emission factor 2) 2 % decarbonization model 3) 5 % decarbonization model	Operating baseline

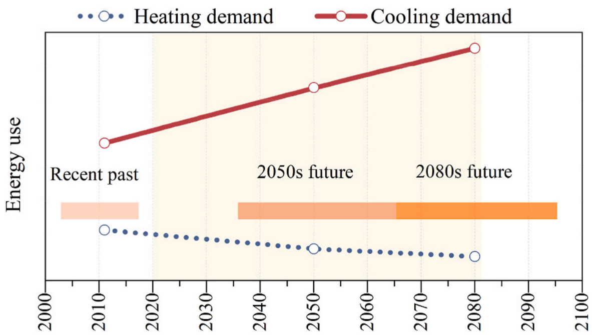

Fig. 3. Evolution model of energy demand for cooling and heating.

$$EU_n = EU_0(1 + g)^n \quad (12)$$

Where EU_n is the annual energy electricity consumption in the n year, EU_0 is the annual energy electricity consumption of the reference year, g is the growth rate, and n is a year counter.

The annual energy demand was comprehensively evaluated across a wide range of scenarios, encompassing 1080 distinct cases that incorporated variations in sandwich panel systems, weather files, climatic zones, and HVAC operational modes. Python was efficiently utilized for batch simulation to handle such a substantial number of cases.

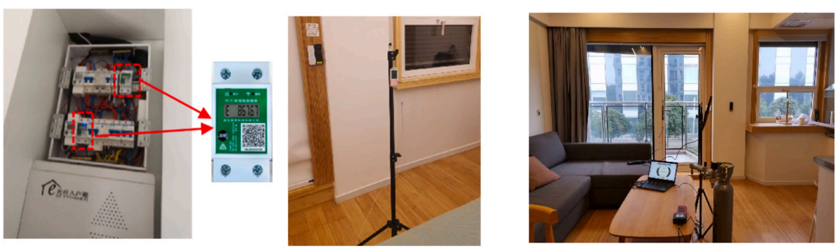

(a) (b) (c)

Fig. 4. (a) Electronic meter used to measure electricity consumption, (b) thermometers used to measure the room air temperature, and (c) tracer gas method used to measure air infiltration rate.

3. Validation

To validate the building energy simulation employed in this research, the HVAC operating baseline in Changsha (HSCW) underwent calibration and validation, through a comparison of simulated and monitored power consumption. The thermometers were used to measure the indoor air temperature, while the tracer gas method was applied to calculate air infiltration rate. These collected data were subsequently used to set up the initial conditions in EnergyPlus. The electrical power consumption was meticulously recorded using an electronic meter. The validation process was conducted over the period spanning from 19:00 on February 4, 2023 to 00:00 on February 9, 2023. Fig. 4 shows these measuring instruments and their placement.

The average indoor air temperature of the whole apartment was 21.2 °C, calculated by the bulk average of the temperatures of the four zones as shown in Fig. S1. The air infiltration was 0.07 air changes per hour, calculated by the standard [42]. These values were used for calibration of the simulation model.

Mean Absolute Error and Root Mean bias error were applied to quantify the agreement between simulated and measured air conditioning power consumption. The average heating Coefficient of performance (COP) of the air conditioning system was 2.8. There was an acceptable level of agreement between the simulated and measured results, as shown in Table 6. The room's human activity, infiltration from open doors, local microclimate, and the efficiency of the actual air conditioning system could affect the difference between the measured and simulated data.

EnergyPlus is a research-grade energy analysis and thermal load modeling program, based on physical principles that has undergone extensive testing and validation over several decades. The validation ins this study also can prove the accuracy of the energy consumption simulation model.

4. Results and discussion

In Section 4.1, the optimal solutions obtained from single-objective analyses focusing on energy, economic, or environmental aspects, as well as from the 3E-objective trade-off analysis, were discussed. This analysis was conducted under the assumption of an operating baseline condition and considering climate change. In Section 4.2, the effect of setting variations in influencing factors, including the HVAC operational mode, energy model, grid emission factor, and building lifespan, on the optimal thickness derived from the 3E-objective optimization method and the life-cycle 3E results were discussed.

4.1. Comparison of optimal solutions based on different methods

Fig. S2-S4 in the SI file graphically illustrate the Pareto frontier solutions obtained from the 3E-objective optimization under the operating baseline condition. Each point corresponds to a design solution for the thickness of external wall. The visual comparison of these solutions provides designers and decision-makers with a comprehensive understanding of the design possibilities and their potential effects. Subsequently, the ideal point method was employed to determine the unique optimal solution of 3E-objective optimization. This solution was then compared with the single-objective optimization solution and the nZEB standard solution, as presented in Fig. 5.

The optimal thickness of external wall varied based on the optimization objectives, which were influenced by the climatic zone and the specific type of sandwich panel system employed. However, these optimization solutions may not fall within the thickness range stipulated by the nZEB standard in some climatic zones, especially when EPS insulation was employed. This was primarily attributed to the diminished thermal mass of the lightweight external wall, as detailed in Table S2 of the SI file. This lead to a more significant deviation from the nZEB standard typically applied to traditional heavyweight external walls. The maximum deviation from nZEB standard reached up to 200 mm at the optimum thickness. This emphasizes the necessity for more comprehensive regulations concerning the identification of lightweight envelopes that are tailored to specific circumstances and require personalized studies.

It was evident in Fig. 5 that optimizing external wall thickness with a priority on carbon emissions reduction typically resulted in greater thickness, whereas prioritizing economic considerations led to thinner optimal thickness. This observation was consistent with previous studies [8]. The difference in optimal thickness was reported, where the thickness for environmental objective was 1–4 times as high as that for the economic one. This differed from the range of 2–8 times reported by Ref. [8]. The difference in the range of optimal thickness between our study and the study by Ref. [8] may be related to the low thermal mass of the lightweight external wall. However, the thickness determined by the 3E-objective method was 1–3.5 times that of the economic one, which varied significantly across different climatic conditions.

Previously, the focus of energy-efficient building design was primarily on minimizing economic considerations. However, the implementation of the national carbon emissions reduction strategy has necessitated a substantial increase in financial investment for carbon emissions reduction, as evidenced in Tables S3–S5 of the SI file. The maximum difference in optimal thickness between

Table 6
Statistical comparison between the simulated and measured power consumption for the validation period

Power consumption (kWh)		Mean Absolute Error (kWh)	Root Mean bias error (%)
Simulated	Measured		
45.47	48.96	−3.49	−7.1

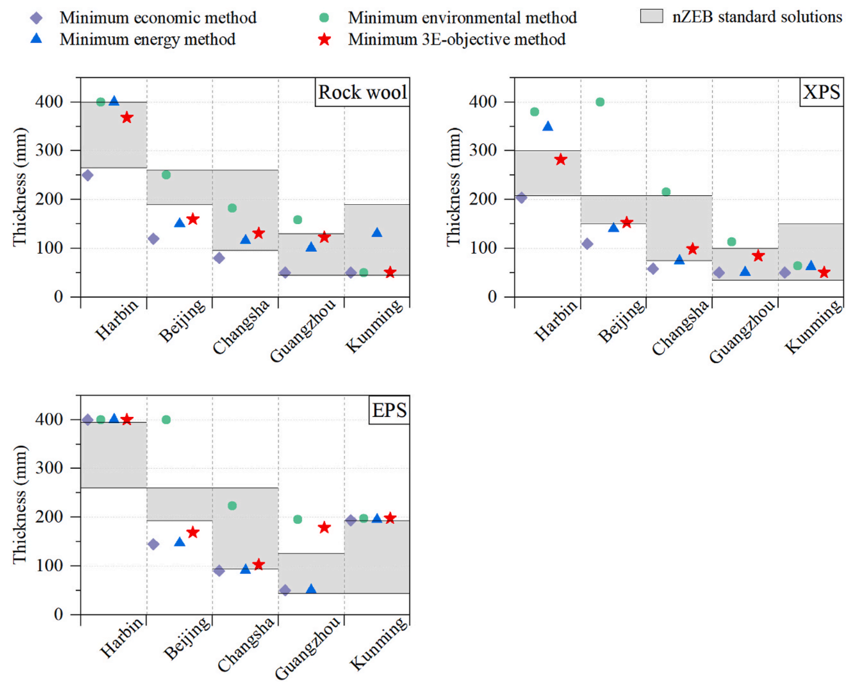

Fig. 5. Minimum single-objective solutions, minimum 3E-objective solutions, and nZEB standard solutions.

environmental and economic objectives reached up to approximately 300 mm, as shown in Fig. 5. This would significantly impact the economic costs, energy consumption, and environmental impact.

The benefit-cost ratio of carbon emissions reduction serves as a comprehensive indicator, quantifying the carbon emissions reduction benefits resulting from increased financial input based on the minimum economic method. The difference in carbon emissions resulting from various objective optimization methods in Kunming (Mild) was negligible, as presented in Tables S3–S5. This indicates that the selection of optimization methods has a relatively minor impact in this climatic zone. This could be attributed to the relatively lower operating energy consumption and reduced grid carbon emission factors within this climatic zone. Table 7 shows the life-cycle benefit-cost ratio of building area per unit for other cities based on minimum environmental, energy, and 3E-objective methods.

Regardless of the optimization method, rock wool exhibited the highest benefit ratio compared to other materials in Harbin (SC), Beijing (Cold), and Changsha (HSCW). In Guangzhou (HSWW), EPS demonstrated the highest benefit ratio. This indicates that these materials provide the most favorable carbon emission reduction benefits for the given increase in economic investment. Notably, the benefit ratio obtained using the 3E-objective method was superior to those using other methods. This comparison further confirmed the rationality and superiority of the 3E-objective optimization method in balancing the economy and carbon emissions.

Table 7
Life-cycle benefit-cost ratio of building area per unit based on minimum environmental, energy, and 3E-objective methods

Cities (Climatic zones)	Optimization method	Benefit-cost ratio of carbon emissions reduction (kg CO2/100 CNY)		
		Rock wool	XPS	EPS
Harbin (SC)	Minimum environmental method	43.8	16.9	–
	Minimum energy method	43.8	22.1	–
	Minimum 3E-objective method	**137.9**	**23.9**	–
Beijing (Cold)	Minimum environmental method	4.4	2.2	4.0
	Minimum energy method	19.3	22.8	–
	Minimum 3E-objective method	**24.1**	**22.7**	**18.2**
Changsha (HSCW)	Minimum environmental method	4.3	1.8	8.2
	Minimum energy method	16.2	8.1	–
	Minimum 3E-objective method	**16.8**	**8.2**	**8.3**
Guangzhou (HSWW)	Minimum environmental method	2.9	2.0	31.7
	Minimum energy method	4.5	–	–
	Minimum 3E-objective method	**4.7**	**3.4**	**42.6**

4.2. Influencing factors affecting 3E-objective optimization solution

This subsection investigates the influence of various influencing factors on the solutions of 3E-objective optimization method. The relative difference (in %) in energy consumption, economic costs, and environmental impact resulting from diverse settings of influencing factors can be calculated by Eq. (13).

$$\%\ change = \left(X_{j,opt,1} - X_{j,opt,2}\right) \cdot 100 / X_{j,opt,2} \tag{13}$$

where $X_{j,opt,1}$ and $X_{j,opt,2}$ are the evaluation parameters (energy consumption, economic costs, or environmental impact) of the optimal solutions in different settings of influencing factors.

4.2.1. HVAC operational mode

Figs. 6 and 7 demonstrate the effect of HVAC operational duration and ventilative cooling strategy on the optimization solutions using the 3E-objective method.

The study found that the optimal thickness of external wall required for an HVAC system in part-time mode was lower than that required for an HVAC system in full-time mode, corroborating the results of Study [14]. Technical standard for nearly zero energy buildings (nZEB) GB/T51350 [21] mandates continuous operation of HVAC systems in residential buildings. However, in practice, particularly in residential buildings such as staff or student apartments, HVAC systems often operate intermittently or are only activated in specific rooms during specific periods. Therefore, applying the optimal external wall thickness calculated for a full-time, as specified by GB/T51350 [21], to a part-time HVAC system would lead to an overestimation of the optimal wall thickness. In Guangzhou (HSWW), it was observed that three sandwich panel systems experienced a reduction of over 40 % in their optimal thickness when the HVAC system operated in part-time mode, compared to the optimal thickness designed for full-time mode (Fig. 6). This discrepancy in optimal thicknesses was expected to increase the life-cycle 3E results, particularly with regards to economic costs which could potentially increase by up to 8.4 % (Fig. 8). This analysis underscores the critical importance for HSWW climatic zones to determine HVAC operational duration as accurately as possible, particularly in economically underdeveloped regions. Increased economic investment does not yield benefits in terms of energy and carbon emissions reduction. In Harbin (SC) and Beijing (Cold), beneficial results in terms of energy and carbon emissions reduction might arise (Fig. 8). This phenomenon mainly occurs as the proportional influence of part-time operation on energy consumption and carbon emissions in relation to full-time operation has increased, leading to a reduction in life-cycle energy consumption and carbon emissions with the increase in thickness. This could be an aspect needing improvement in this research method for subsequent studies. The unique optimal solution of 3E-objective optimization failed to consider the disparities in the economy and the demands for carbon emission reduction among different regions.

In the optimization of external wall design, the critical role of ventilative cooling was often neglected. This neglect can lead to excessively thick walls in Guangzhou (HSWW), thereby imposing unnecessary life-cycle economic costs, reaching a maximum of 5.1 % (Fig. 8). But this neglect in design does not necessarily result in increased energy consumption or carbon emissions. Conversely, in Harbin (SC) and Beijing (Cold), the optimal thickness may be slightly underestimated; however, this effect of less than 1 % was almost negligible (Fig. 8). Overall, across all climatic zones, the influence of ventilative cooling technology on the optimal thickness of external wall does not exhibit a consistent trend of increase or decrease. This trend primarily depended on the specific climate zone and the type of wall selected. Additionally, the variability in optimal thickness and its impact on life-cycle 3E results were diverse.

4.2.2. Energy model

In this section, the optimal thickness of external wall was compared using a static energy model, with that obtained from a dynamic energy model, as illustrated in Fig. 9.

The traditional static energy model has overlooked the effect of climate change on energy consumption [43]. The optimal thickness of external wall obtained by the simplified static energy model was greater than that obtained by the dynamic energy model. The finding was coherent with the results reported by Ref. [18], which were determined solely from an economic standpoint. This

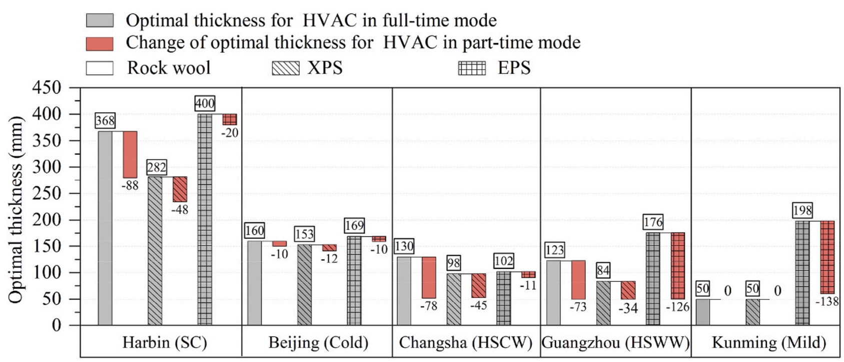

Fig. 6. Optimal thickness of external wall for the condition with the HVAC system in full-time mode or part-time mode.

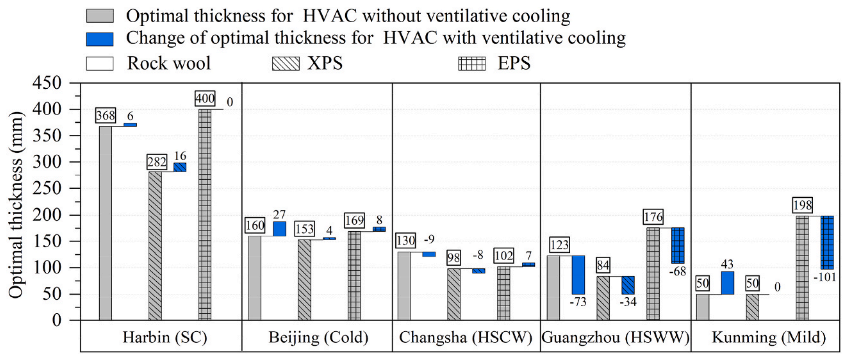

Fig. 7. Optimal thickness of external wall for the condition with or without ventilative cooling strategy.

discrepancy can be primarily attributed to the increased demand for enhanced heat dissipation capacity from the wall due to climate warming. The increase in the optimal thickness was dependent on the insulation material used and the climatic zone, and can be increased up to 1.4 times (rock wool in Kunming (Mild)). While this increase led to a rise in life-cycle economic costs, such a rise would not exceed 2 % (Fig. 8). An increase in economic costs may be exchanged for lower energy or carbon emissions. Importantly, this study was based on future weather scenarios under the SSP5-8.5 pathway which often represents a "business-as-usual" trajectory assuming a high carbon emissions scenario. Under alternative scenarios with lower emissions, both optimal thickness and corresponding life-cycle 3E results were expected to decrease. Therefore, the effect of climate change on the optimal thickness of external wall was relatively modest.

4.2.3. Grid emission factor

Fig. 10 displays the optimal thickness of external wall for static and dynamic grid emission factors. The grid emission factor is commonly assumed to be constant when assessing building carbon emissions. However, the future timeline for electrification and decarbonization would impact the trade-offs between building embodied and operational carbon emissions, thereby influencing the optimal thickness of external wall. If the optimal thickness had been designed based on a static grid emission factor, without considering the potential dynamic decarbonization rate of grid power, then the designed optimal thickness of external wall would be overestimated. This finding was consistent with previous study [9]. This phenomenon can primarily be attributed to the dynamic grid emission factor placing greater emphasis on embodied carbon emissions, consequently leading to a reduction in the optimal thickness of external wall. However, given the differences between the optimization objectives and building objects adopted in this study and in Ref. [9], a discrepancy in the extent of reduction was observed. Considering the same 5 % decarbonization model, in the study of [9], the optimal thickness of EPS is reduced from 105 mm in the static scenario to 35 mm and XPS is reduced from 95 mm to 65 mm in HSCW zone. In this study, the optimal thickness of EPS is reduced from 102 mm in the static scenario to 90 mm and XPS is reduced from 98 mm to 59 mm in HSCW zone. This variation in the magnitude of reduction can likely be attributed to differences in the construction of external walls and the optimization methodologies used.

When operating in a realistic dynamic scenario, the optimization of external wall thickness neglecting the variations of the future electricity mix will inevitably increase the life-cycle economic costs, but it may have a positive effect on reducing energy consumption and carbon emissions. When grid carbon reduction policies are implemented more quickly, for instance from a 2 % decarbonization rate to a 5 % decarbonization rate, the optimal thickness will be further decreased, and the beneficial effect of reducing energy consumption and carbon emissions may also be turned into a negative effect (Fig. 8).

4.2.4. Building lifespan

Fig. 11 illustrates the optimal thickness of external wall for buildings with different lifespans. The majority of life-cycle assessment studies typically assumed a standardized building lifespan for each major structural type. However, the actual service life of buildings varies significantly due to various factors such as building materials, construction quality, maintenance practices, and environmental conditions. Previous research [8] has shown that extending a building's lifespan from 20 to 50 years required an average increase ranging from 60 % to 90 % in the optimal thickness of external walls to attain the best economic performance. However, this finding was based on the assumption that the insulation material also had a lifespan matching the building's lifespan. This study specifically considered the necessity of replacing insulation every 20 years. Contrary to the finding of the research [8], to extend the life of the building from 20 years to 40 years, the optimal thickness could decrease by up to 150 %, and to extend it to 60 years, the optimal thickness could decrease by up to 190 %, as was evident from Fig. 11. This phenomenon can primarily be attributed to the extended lifespan of buildings, which leads to an increase in the embodied economic costs that outweighs the reduction in operational economic costs as thickness increases. Consequently, the optimal thickness shifted towards a lower embodied economic costs. Buildings that did not adhere to their designed long life cycle will not only escalate the life-cycle economic costs but also lead to increased carbon emissions across most climatic zones (Fig. 8). Therefore, it is crucial to consider the building's lifespan more accurately during the architectural design process.

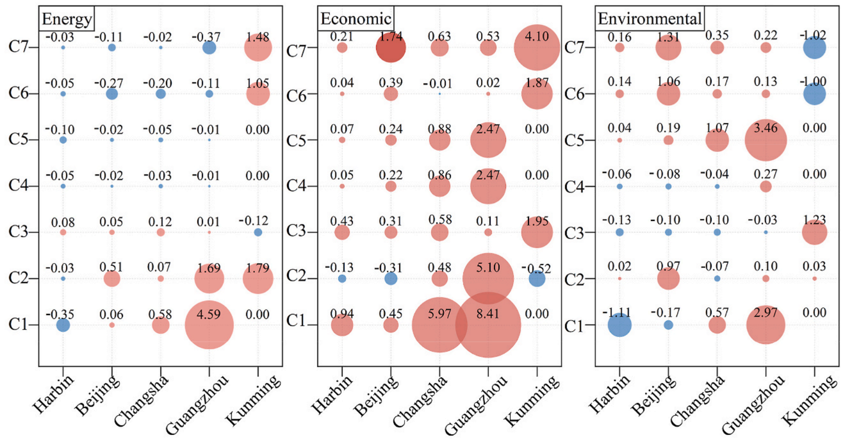

a) Rock wool

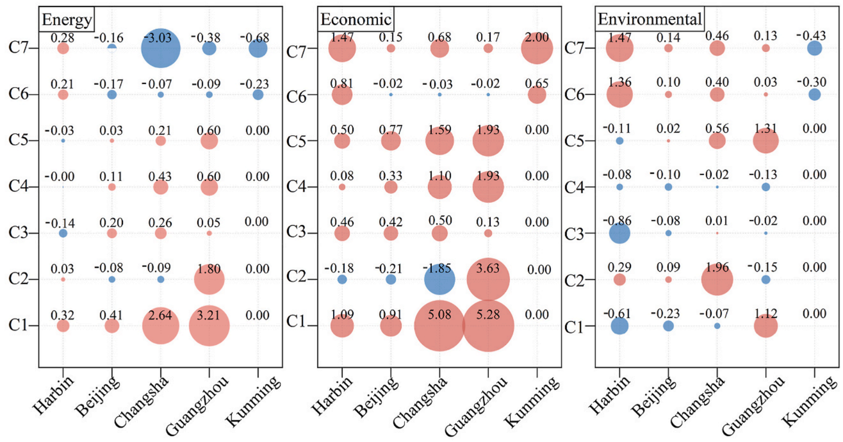

b) XPS

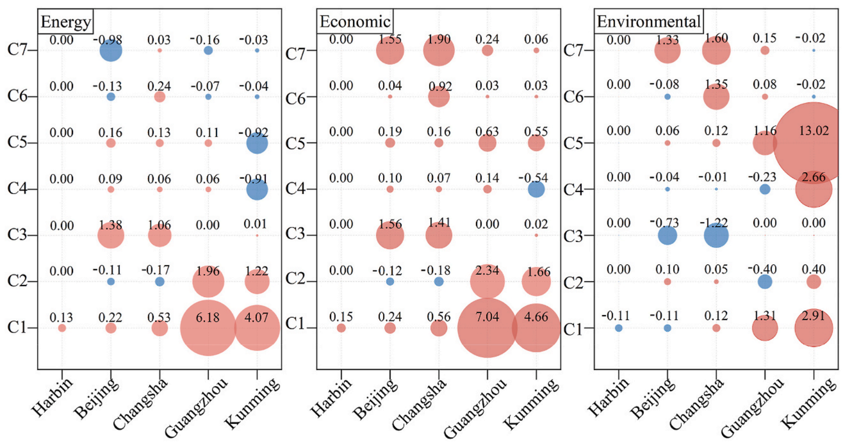

c) EPS

Fig. 8. Relative difference in life-cycle energy consumption, economic costs, and environmental impact resulting from various settings of influencing factors for (a) Rock wool (b) XPS (c)EPS. (C1: HVAC in full-time operational mode compared to part-time operational mode; C2: HVAC in full-time operational mode without ventilative cooling compared to that with ventilative cooling; C3: Static energy model compared to dynamic energy model; C4, C5: static grid emission factor compared to 2 % and 5 % decrease in grid emission factor; C6, C7: 60-year building lifespan compared to 40-year and 20-years. Blue bubbles indicate negative effects and red bubbles indicate positive effects.)

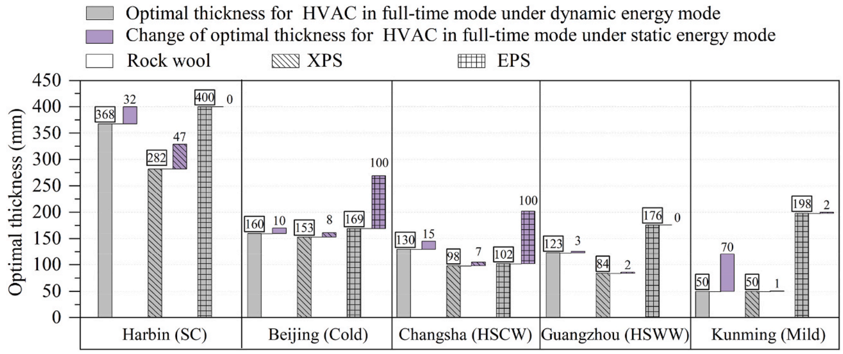

Fig. 9. Optimal thickness of external wall for the condition with dynamic or static energy model.

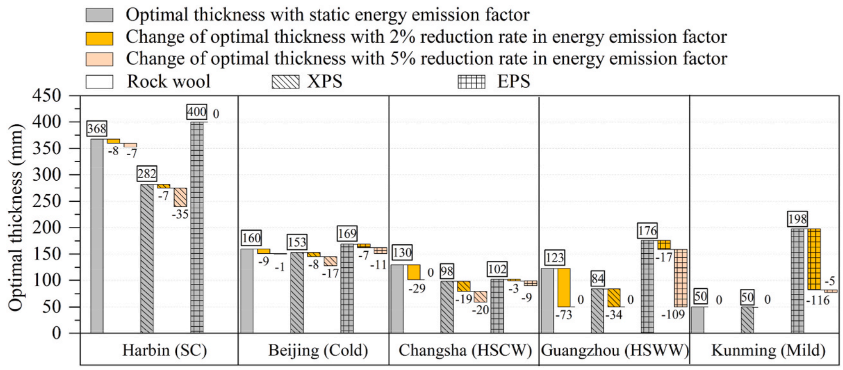

Fig. 10. Optimal thickness of external wall for the condition with dynamic or static grid emission factor.

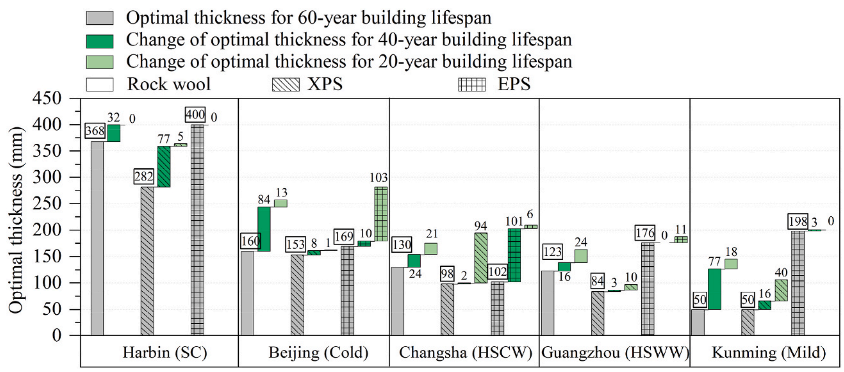

Fig. 11. Optimal thickness of external wall for the condition with different building lifespans.

5. Limitations and future outlook

The 3E-objective optimization method used in this study maintains equal weights for its objectives, aiming to achieve a balance among all the objectives. However, it is important to note that this approach may not always align with the actual preferences of decision makers. The exploration of the effects of the optimization results with diverse weights and the uncertainty of parameter settings on the optimization results has not been conducted. In practical applications, decision makers may necessitate adjusting these weights on a case-by-case basis to accurately reflect the relative importance of different objectives. Therefore, future studies should consider conducting sensitivity analyses on weights to investigate the effect of different weight combinations on parameter settings and optimization outcomes across diverse policy scenarios. This would provide a more comprehensive understanding of the significance of parameter settings.

Additionally, the present calculations in this study do not consider the practical challenges related to the suitability or incompatibility of sandwich panel systems for specific building types. In reality, it is imperative to thoroughly evaluate factors such as their applicability to installation procedures, load-bearing capacity, acoustic control requirements, and other practical considerations.

6. Conclusions

This study compares the optimal thickness of lightweight Modular Integrated Construction (MIC) external wall obtained using the single-objective method and the multi-objective method, considering building life-cycle energy consumption, economic costs, and carbon emissions as objective functions. Then, it explores the influence of multiple factors on the multi-objective optimization results, including the choice of HVAC system operational mode, future climate change scenarios, changes in grid carbon emission factors, and the determination of the building's expected service life.

Lightweight external wall designed in accordance with current energy efficiency standards may not be optimal, whether based on a single objective of minimizing energy, economy, or environment (3E), or multiple objectives encompassing these three aspects. As the thermal mass of external wall decreases, the optimal thickness will deviate further from the thickness specified by energy efficiency standards. There is a need for new regulations to determine lightweight external wall designs that are suitable for specific objectives.

The application of the NSGA-II optimization method in conjunction with the ideal point method has demonstrated remarkable performance in determining the optimal thickness to achieve the highest cost-benefit ratio in carbon emission reduction, outperforming traditional energy or environmental approaches. Among insulation materials, rock wool presented the highest cost-benefit ratio in SC, Cold, and HSCW zones, while EPS manifested the highest cost-benefit ratio in HSWW zone.

The study reveals the effects of building operating parameter settings and climate change on the results obtained when determining the optimal wall thickness. Applying thickness values optimized for full-time HVAC systems according to energy efficiency standards to non-full-time HVAC systems results in overestimation, with the HSWW zone experiencing the most significant increase in the life-cycle 3E results, while SC and Cold zones show either negligible impacts or even reductions in life-cycle energy consumption and carbon emissions. The static energy model yields higher optimal thickness compared to the dynamic energy model. Despite its inherent limitations, the marginal deviation in life-cycle 3E results suggests that the static energy model retains practical utility for preliminary design. Neglecting grid decarbonization trajectories leads to thickness overestimation, which elevates life-cycle economic cost. This overestimation may reduce carbon emissions in some climatic zones but can increase them when grid decarbonization is accelerated. The optimal thickness is reduced as the building lifespan is extended from 20 to 60 years, when taking into account the current limited lifespan of insulation. This finding contrasts with the scenario where the insulation's lifespan is assumed equivalent to that of the building.

CRediT authorship contribution statement

Yan Hu: Writing – original draft, Validation, Software, Methodology, Formal analysis, Data curation. **Zhengtao Ai:** Writing – review & editing, Supervision, Project administration, Methodology. **Guoqiang Zhang:** Resources, Funding acquisition. **Jie Zong:** Writing – review & editing. **Zhengxuan Liu:** Writing – review & editing, Conceptualization.

Declaration of competing interest

The authors declare that they have no known competing financial interests or personal relationships that could have appeared to influence the work reported in this paper.

Acknowledgments

The authors would like to express their gratitude to the Broad Group for providing the information about the MIC case.

Appendix A. Supplementary data

Supplementary data to this article can be found online at https://doi.org/10.1016/j.jobe.2025.112090.

Data availability

Data will be made available on request.

References

[1] Global Status Report for Buildings and Construction - beyond Foundations: Mainstreaming Sustainable Solutions to Cut Emissions from the Buildings Sector." (accessed July, 2024).
[2] X. Su, S. Tian, X. Shao, X. Zhao, Embodied and operational energy and carbon emissions of passive building in HSCW zone in China: a case study, Energy Build. 222 (2020/09/01/2020) 110090, https://doi.org/10.1016/j.enbuild.2020.110090.
[3] M.K. Akyüz, Enviroeconomic optimization of insulation thickness for building exterior walls through thermoeconomic and life cycle assessment analysis, Case Stud. Therm. Eng. 65 (2025/01/01/2025) 105606, https://doi.org/10.1016/j.csite.2024.105606.

[4] M. Ashouri, F.R. Astaraei, R. Ghasempour, M.H. Ahmadi, M. Feidt, Optimum insulation thickness determination of a building wall using exergetic life cycle assessment, Appl. Therm. Eng. 106 (2016/08/05/2016) 307–315, https://doi.org/10.1016/j.applthermaleng.2016.05.190.
[5] A. Bolattürk, Optimum insulation thicknesses for building walls with respect to cooling and heating degree-hours in the warmest zone of Turkey, Build. Environ. 43 (6) (2008/06/01/2008) 1055–1064, https://doi.org/10.1016/j.buildenv.2007.02.014.
[6] S.A. Al-Sanea, M.F. Zedan, S.A. Al-Ajlan, Effect of electricity tariff on the optimum insulation-thickness in building walls as determined by a dynamic heat-transfer model, Appl. Energy 82 (4) (2005/12/01/2005) 313–330, https://doi.org/10.1016/j.apenergy.2004.10.014.
[7] E. Amiri Rad, E. Fallahi, Optimizing the insulation thickness of external wall by a novel 3E (energy, environmental, economic) method, Constr. Build. Mater. 205 (2019/04/30/2019) 196–212, https://doi.org/10.1016/j.conbuildmat.2019.02.006.
[8] J. Barrau, M. Ibañez, F. Badia, Impact of the optimization criteria on the determination of the insulation thickness, Energy Build. 76 (2014/06/01/2014) 459–469, https://doi.org/10.1016/j.enbuild.2014.03.017.
[9] C. Li, et al., Optimal design of building envelope towards life cycle performance: impact of considering dynamic grid emission factors, Energy Build. 323 (2024/11/15/2024) 114770, https://doi.org/10.1016/j.enbuild.2024.114770.
[10] T. Méndez Echenagucia, T. Moroseos, C. Meek, On the tradeoffs between embodied and operational carbon in building envelope design: the impact of local climates and energy grids, Energy Build. 278 (2023/01/01/2023) 112589, https://doi.org/10.1016/j.enbuild.2022.112589.
[11] S. Motaghian, M.H. Monajati Saharkhiz, S. Rayegan, H. Pasdarshahri, P. Ahmadi, M.A. Rosen, Techno-economic multi-objective optimization of detailed external wall insulation scenarios for buildings in moderate-dry regions, Sustain. Energy Technol. Assessments 46 (2021) 101256, https://doi.org/10.1016/j.seta.2021.101256. (Accessed 8 January 2021).
[12] C. Wu, H. Pan, Z. Luo, C. Liu, H. Huang, Multi-objective optimization of residential building energy consumption, daylighting, and thermal comfort based on BO-XGBoost-NSGA-II, Build. Environ. 254 (2024/04/15/2024) 111386, https://doi.org/10.1016/j.buildenv.2024.111386.
[13] Z. Li, Y. Zhao, H. Xia, S. Xie, A multi-objective optimization framework for building performance under climate change, J. Build. Eng. 80 (2023/12/01/2023) 107978, https://doi.org/10.1016/j.jobe.2023.107978.
[14] E. Tunçbilek, A. Komerska, M. Arıcı, Optimisation of wall insulation thickness using energy management strategies: Intermittent versus continuous operation schedule, Sustain. Energy Technol. Assessments 49 (2022/02/01/2022) 101778, https://doi.org/10.1016/j.seta.2021.101778.
[15] L. Yuan, R. Wang, X. Zhu, Y. Lu, Optimum configuration of internal walls in intermittently conditioned rooms with different ventilation-behavior during off-periods and air conditioner operation durations, Energy 309 (2024/11/15/2024) 133065, https://doi.org/10.1016/j.energy.2024.133065.
[16] K. Verichev, M. Zamorano, A. Fuentes-Sepúlveda, N. Cárdenas, M. Carpio, Adaptation and mitigation to climate change of envelope wall thermal insulation of residential buildings in a temperate oceanic climate, Energy Build. 235 (2021/03/15/2021) 110719, https://doi.org/10.1016/j.enbuild.2021.110719.
[17] J.E. Gaarder, N.K. Friis, I.S. Larsen, B. Time, E.B. Møller, T. Kvande, Optimization of thermal insulation thickness pertaining to embodied and operational GHG emissions in cold climates – future and present cases, Build. Environ. 234 (2023/04/15/2023) 110187, https://doi.org/10.1016/j.buildenv.2023.110187.
[18] Y. Kharbouch, H. Boushaba, M. Ameur, Optimisation of the insulation thickness for the external walls in Morocco while considering the effect of climate change, Therm. Sci. Eng. Prog. 35 (2022) 101455, https://doi.org/10.1016/j.tsep.2022.101455. (Accessed 10 January 2022).
[19] X. Su, Y. Huang, C. Chen, Z. Xu, S. Tian, L. Peng, A dynamic life cycle assessment model for long-term carbon emissions prediction of buildings: a passive building as case study, Sustain. Cities Soc. 96 (2023/09/01/2023) 104636, https://doi.org/10.1016/j.scs.2023.104636.
[20] S. Naji, L. Aye, M. Noguchi, Multi-objective optimisations of envelope components for a prefabricated house in six climate zones, Appl. Energy 282 (2021/01/15/2021) 116012, https://doi.org/10.1016/j.apenergy.2020.116012.
[21] *Technical Standard for Nearly Zero Energy Buildings*, M. O. H. a. H.-R. D. O. T. P. S. R. O. C. GB/T51350, 2019.
[22] S. Attia, M. Hamdy, W. O'Brien, S. Carlucci, Assessing gaps and needs for integrating building performance optimization tools in net zero energy buildings design, Energy Build. 60 (2013/05/01/2013) 110–124, https://doi.org/10.1016/j.enbuild.2013.01.016.
[23] Y. Teng, K. Li, W. Pan, T. Ng, Reducing building life cycle carbon emissions through prefabrication: evidence from and gaps in empirical studies, Build. Environ. 132 (2018/03/15/2018) 125–136, https://doi.org/10.1016/j.buildenv.2018.01.026.
[24] T. Vasishta, M. Hashem Mehany, J. Killingsworth, Comparative life cycle assesment (LCA) and life cycle cost analysis (LCCA) of precast and cast–in–place buildings in United States, J. Build. Eng. 67 (2023/05/15/2023) 105921, https://doi.org/10.1016/j.jobe.2023.105921.
[25] S. Abdelmageed, T. Zayed, A study of literature in modular integrated construction - critical review and future directions, J. Clean. Prod. 277 (2020/12/20/2020) 124044, https://doi.org/10.1016/j.jclepro.2020.124044.
[26] A. Al-Najjar, A. Dodoo, Modular multi-storey construction with cross-laminated timber: life cycle environmental implications, Wood Mater. Sci. Eng. 18 (2) (2023/03/04 2023) 525–539, https://doi.org/10.1080/17480272.2022.2053204.
[27] A. Dodoo, L. Gustavsson, R. Sathre, Lifecycle carbon implications of conventional and low-energy multi-storey timber building systems, Energy Build. 82 (2014/10/01/2014) 194–210, https://doi.org/10.1016/j.enbuild.2014.06.034.
[28] K. Cai, et al., Mitigating lifecycle GHG emissions of building sector through prefabricated light-steel buildings in comparison with traditional cast-in-place buildings, Resour. Conserv. Recycl. 194 (2023) 107007, https://doi.org/10.1016/j.resconrec.2023.107007. (Accessed 1 July 2023).
[29] Y. Hu, Z. Ai, P. Wargocki, Y. Chang, G. Zhang, Ventilative cooling of residential buildings in China: a simulation-based evaluation of lightweight modular integrated constructions considering climate change, Energy Build. 317 (2024/08/15/2024) 114382, https://doi.org/10.1016/j.enbuild.2024.114382.
[30] E. Yılmaz, B. Aykanat, B. Çomak, Environmental life cycle assessment of rockwool filled aluminum sandwich facade panels in Turkey, J. Build. Eng. 50 (2022) 104234, https://doi.org/10.1016/j.jobe.2022.104234. (Accessed 6 January 2022).
[31] V. Birman, G.A. Kardomateas, Review of current trends in research and applications of sandwich structures, Compos. B Eng. 142 (2018/06/01/2018) 221–240, https://doi.org/10.1016/j.compositesb.2018.01.027.
[32] K. Biswas, S.S. Shrestha, M.S. Bhandari, A.O. Desjarlais, Insulation materials for commercial buildings in North America: an assessment of lifetime energy and environmental impacts, Energy Build. 112 (2016/01/15/2016) 256–269, https://doi.org/10.1016/j.enbuild.2015.12.013.
[33] R. Minunno, T. O'Grady, G.M. Morrison, R.L. Gruner, Investigating the embodied energy and carbon of buildings: a systematic literature review and meta-analysis of life cycle assessments, Renew. Sustain. Energy Rev. 143 (2021/06/01/2021) 110935, https://doi.org/10.1016/j.rser.2021.110935.
[34] T. Zheng, L. Gong, S. Ye, Global energy market connectedness and inflation at risk, Energy Econ. 126 (2023/10/01/2023) 106975, https://doi.org/10.1016/j.eneco.2023.106975.
[35] NDRC. "TheGlobalEconomy.com." National Development and Reform Commission https://zh.globalpetrolprices.com/China/electricity_prices/(accessed 17th, 6, 2024).
[36] Y. Zhu, F. Zhang, S. Jia, Embodied energy and carbon emissions analysis of geosynthetic reinforced soil structures, J. Clean. Prod. 370 (2022/10/10/2022) 133510, https://doi.org/10.1016/j.jclepro.2022.133510.
[37] 000014672/2024-00149, CO_2 emission factors for electricity in 2021 [Online] Available: https://www.mee.gov.cn/xxgk2018/xxgk/xxgk01/202404/t20240412_1070565.html, 2024.
[38] The Reference Comprehensive Unit Price for the Bill of Quantities, 2024.
[39] General Code for Energy Efficiency and Renewable Energy Application in Buildings, 2021. GB/T55015.
[40] E. Rodrigues, M.S. Fernandes, D. Carvalho, Future weather generator for building performance research: an open-source morphing tool and an application, Build. Environ. 233 (2023) 110104, https://doi.org/10.1016/j.buildenv.2023.110104. (Accessed 4 January 2023).
[41] D. Ramon, K. Allacker, D. Trigaux, H. Wouters, N.P.M. van Lipzig, Dynamic modelling of operational energy use in a building LCA: a case study of a Belgian office building, Energy Build. 278 (2023/01/01/2023) 112634, https://doi.org/10.1016/j.enbuild.2022.112634.
[42] Standard Test Method for Determining Air Change in a Single Zone by Means of a Tracer Gas Dilution, 2017. A. E741-11.
[43] W.O. Collinge, A.E. Landis, A.K. Jones, L.A. Schaefer, M.M. Bilec, Dynamic life cycle assessment: framework and application to an institutional building, Int. J. Life Cycle Assess. 18 (3) (2013/03/01 2013) 538–552, https://doi.org/10.1007/s11367-012-0528-2.